JOURNAL OF AGRICULTURAL AND FOOD CHEMISTRY



# Nutriomic Analysis of Fresh and Processed Fruit Products. 2. During in Vitro Simultaneous Molecular Passages Using Caco-2 Cell Monolayers

INDAH EPRILIATI,*,† BRUCE D'ARCY,† AND MIKE GIDLEY§

School of Land, Crop and Food Sciences and Center for Nutrition and Food Sciences, The University of Queensland, Slip Road, St. Lucia, Australia 4072

Many studies have used Caco-2 cell monolayers as human intestinal absorption models. However, only a few studied digested foods, instead of pure standard compounds. Moreover, beneficial and nutritional molecules (nutriome) have not been investigated simultaneously. The present study explored nutriome passages from digest solution of fresh, dried, and juiced tomato, mango, and papaya using Caco-2 cell monolayers in apical→basolateral directions. A validation method using complementary TEER and $P_{app}$ values or internal standard caffeine is recommended because physiologically passive diffusion is unlikely to happen. Sugars were transported into basolateral sides, resulting in potential glucose equivalent bioavailability of 2.26−75 mg $h^{-1}$/100 g (WB). Using sugar passage rates (DB) of juices as 100% references, the rate order was tomato (49.8% dried; 89.5% fresh) > mango (56.8% dried; 22.8% fresh) > papaya (18.7% dried; 36.7% fresh). Major indications that phytochemical absorption does not occur in the small intestine were obtained from the bioassay condition selected. Apical organic acid levels decreased, which occasionally were transported into basolateral sides, whereas the disappearances of apical carotenoids and phenolics were not. Pectin substances were predicted to be responsible for the disappearances of bioactive compounds in those pectin-rich fruits. Further investigations on the role of pectin substances in intestinal passages are recommended.

**KEYWORDS: Nutriomic analysis; fresh and processed fruits; in vitro passage; Caco-2 monolayers; tomato; mango; papaya**

## INTRODUCTION

This second in a pair of papers discusses nutriomic analysis at absorption stage using a Caco-2 monolayer for in vitro bioavailability measurements. In vitro data are useful for studies that cannot be directly carried out in human subjects such as beneficial food components required for maintaining human health. Currently, cancerous cell lines are the best approach accepted to solve this problem. In addition, investigation on bioavailability at particular levels cannot be carried out using in vivo studies due to species differences, high cost, and time. Moreover, these in vivo methods are not practical for routine measurements, for example, in evaluating health food product development. In addition, the animal model surrogates do not have physiological aspects similar to those of humans. Therefore, an in vitro model needs to be tested especially for assessing efficacy of functional foods.

Bioavailability of ingested food components is frequently measured as the plasma level. A study tracing the beneficial compounds from kale (*Brassica oleracea*) via plasma level indicated the appearance of lutein and phylloquinone at 8 h after consumption and $\beta$-carotene and retinol formation at 24 h after consumption (*1*). Interestingly, there were successive peaks for individual compounds at 7 h (phylloquinone, 3 nM), 11 h (lutein, 0.23 $\mu$M), and 24 h (retinol, 0.1 $\mu$M); surprisingly, $\beta$-carotene had a double peak at 8 h (0.058 $\mu$M) and 24 h (0.062 $\mu$M). The retinol formation data were reproducible when the kale study monitored $^{13}$C-labeled nutrients (*2*). Another study using papaya showed that both esterified and nonesterified $\beta$-cryptoxanthin are absorbed, with plasma levels reaching a maximum at 6−12 h, probably involving deesterification enzymes in the gut (*3*). In contrast, plasma levels of phenolics left metabolites disputed for unclear conjugated forms (*4, 5*) and studies of the glycemic index are known to be compounded by C-protein levels (*6*).

* Address correspondence to this author at Food Technology, Widya Mandala Surabaya Catholic University, Jl. Dinoyo 42−44 Surabaya, Indonesia 60265 (telephone +62 31 5678478, ext. 146; fax +62 31 5610818; e-mail margarethaiev@gmail.com).

† School of Land, Crop and Food Sciences.

§ Center for Nutrition and Food Sciences.

10.1021/jf802226n CCC: $40.75 
Published on Web 03/16/2009

This suggested that in vivo bioavailability is variable and that there is an inter-related action to exert benefits on human well-being.

Intensive studies on the use of Caco-2 cell monolayers as a mimetic model for human absorptive tissues suggest that the cell line is applicable for a range of target nutriome components: carotenoids (*7*−*15*), phenolics (*16*−*23*), minerals (e.g., iron) and affecting factors (e.g., organic acids, ascorbic acid, and anti-nutrition phytic acid) (*23*−*44*), and sugar transporters (*45*). Because enterocytes are living cells, they can also metabolize and transport nutrients. This may be beneficial for producing appropriate molecular forms of the nutrients required in the human circulatory system (*46*−*53*). However, current bioavailability models determine only the compounds that are found in the food consumed, whereas metabolites that may be generated during digestion are overlooked.

Particular attention was paid for postabsorption of lipids and fat-soluble components. Individual transport of fat-soluble compounds has been reported, for instance, absorption of vitamin E (*54*−*57*) and carotenoids (*58*−*61*). However, the role of lipids in the absorption of fat-soluble nutriome needs more evaluation. Although fat intake is generally recommended to be reduced, a small amount of fat in the diet is necessary to facilitate uptake of components such as carotenoids (*62*). It may be not only lipid that is important in carotenoid uptake, but also emulsifier in the diets such as protein (*50*, *61*−*63*).

Why is the recommendation of increasing fruit consumption not accompanied with an increased oil/fat intake if this is known to be better? Research in this area is limited; thus, investigating carotenoid behavior during digestion in an environment without additional coconsumed lipids may fill the gap. Is the human small intestine the main site for bioactive compound absorption, or is it important that some nutrients survive to the colon for metabolism and uptake?

Recent findings show involvement of scavenger class B type I (SR-BI) in lipid and insulin regulation (*60*, *61*, *63*−*69*). Current research suggests that SR-BI has an indirect role (*64*) in lipophilic component transports (most studies are for cholesterol) and apolipoprotein synthesized from oxidized fatty acids (*68*). The activity of SR-BI in pancreas dysfunction and a relationship with insulin secretion by $\beta$-cells affected by VLDL and HDL are also found (*69*). In line with this, in carotenoid transports using Caco-2 cells, During et al. (*61*) and During and Harisson (*62*) proposed that the transports may require more than one transporter for facilitated transports.

Few of the previous studies used whole food digest solutions; targets were mostly single compounds or related groups of compounds. In the human intestinal brush border, all nutriome components are absorbed simultaneously from the chyme. Therefore, the present project approach was to develop a model based on the simultaneous absorption of components found in the human digestive system. The developed in vitro absorptive model was applied to digest solutions from fruits containing various nutriome components, including sugars, organic acids, and bioactive phenolics and carotenoids.

## MATERIALS AND METHODS

**Materials.** *Chemicals.* Atenolol, caffeine, caffeic acid, *p*-coumaric acid, *o*-coumaric acid, mangiferin, chlorogenic acid, ferulic acid, fumaric acid, naringenin, hydroxybenzeoic acid, (+)-catechin, succinic acid, *trans*-aconitic acid, malonic acid, malic acid, citric acid, oxalic acid, L-ascorbic acid, tartaric acid, *tert*-butyl methyl ether (MTBE), $\beta$-carotene, retinol synthetic, 13-*cis*-retinol, retinal, and retinoic acid, Dowex 1x8 chloride form 100−200 mesh, Dowex 50Wx8 hydrogen form 100−200 mesh, $^{14}$C-mannitol, lycopene, *all-trans*-retinol, Hank's Buffer Salt Solution (HBSS), 0.025% trypsin−EDTA solution, 0.02% EDTA solution, and DMSO (cell culture grade) were from Sigma-Aldrich; Chelex 100 was from Bio-Rad. Lutein and $\beta$-cryptoxanthin were from Extrasynthese, and Optivin enzyme mix, that is, a mixture of pectinase, hemicellulase, cellulase, and protease (Enzyme Solution Pty, Ltd.) was used. Nitrocellulose filter membranes 0.45 $\mu$m, nylon filter membranes 0.45 and 0.2 $\mu$m, plastic syringes 1−10 mL, and SePack solid-phase extraction cartridges were from Phenomenex; weak cation exchange (WCX)-Oasis cartridges (Waters) and 50 mL Falcon tubes were consumables required in this method development. $C_{18}$ powder was from Alltech. High glucose containing sodium pyruvate and phenol red Dulbeco's Modified Eagle Media (DMEM), nonessential amino acid solution (NEA), fetal bovine serum (FBS), and 1 M HEPES [4-(2-hydroxylethyl)-1-piperazineethanesulfonic acid] solution were all obtained from Invitrogen; penicillin−streptomycin 1000 U−1000 mg/mL was obtained from Biowithaker.

**Methods.** *Caco-2 Cell Bioassay Control Experiments.* Blank buffer controls for the Caco-2 cell bioassays were carried out. HBSS−25 mM HEPES buffer solutions were subjected to Caco-2 monolayer treatment similar to that for the samples. No phenolics or carotenoids were detected during chemical analysis of the HBSS−25 mM HEPES; peak/noise ratios >10 were set as the limit of detection for the organic acid analysis, because bile acids can interfere with the organic acid separation. HBSS−25 mM HEPES contained 8 mg/mL glucose ($4.4 \times 10^4$ nmol/mL) for cell viability during the bioassay; in this study, quantification of basolateral glucose levels was corrected to take into account this buffer glucose level.

*Culturing Frozen Cells.* Culture stock was thawed in a 37 °C water bath for a maximum of 2 min. After removal of the cyro-preservative medium containing 10% DMSO, the cells was seeded into 25 mL T-flasks (Nunc) using DMEM containing 20% FBS and 0.5% NEA. Media were renewed every 2 days. Every time the cultures were reseeded in a new flask, passage numbers (common term for the generation number) were recorded, because as the passage number increases, the cell line can physiologically change, causing different bioassay performances.

*Maintaining Cultures.* After the thawed culture reached confluency (the monolayers cover the growing surface areas), the cells were split into new flasks using DMEM containing 10% FBS and 0.5% NEA, before transferring them into a 24 transwell insert plate having a 0.33 $cm^2$ polycarbonate membrane area each. All biosafety-related works were carried out in a Gelaire Biosafety Cabinet Class II (The Kelly Co. Pty, Ltd.). When the culture reached about 80% confluence, the cell cultures were detached with a 0.25% EDTA−trypsin solution and incubated at 37 °C; the cell suspensions were centrifuged at 1000 rpm to collect cell pellets. Single cells were obtained through gentle aspirations with a fine pipet electronically. Single-cell suspensions containing ca. $10^5$ cells were seeded into each transwell insert. Cell counting was carried out using a hematocytometer counter under a light microscope. The glass object in the hematocytometer has 1 $mm^2$ grid-lined areas representing $10^{-4}$ mL of cell suspensions. Cells were counted from two to four squares depending on the cell densities. Cell numbers (cells/mL) were determined as average cell numbers $\times 10^{-4}$. The medium for the well plate culture was 10% FBS, 0.5% NEA, and 0.5% penicillin−streptomycin. Cells were grown in an autoflow $CO_2$ air-jacketed incubator (NU-5510E Nuaire DHD Autoflow $CO_2$ air-jacketed incubator; Nuaire, Inc.) with an atmosphere of 5% $CO_2$ and 95% relative humidity for 21−22 days before being used in the bioassays. A 24-well plate was chosen for good uniformity of cell monolayers. The heterogeneity of the Caco-2 cell monolayers was determined using a light microscope. It shows typical monolayers, where the following are evident: (a) smooth dense monolayers; (b) smooth monolayers composed of large and less dense cells; and (c) possible higher topography of domes.

*Transepithelial Electrical Resistance (TEER) Measurements.* A Millicell-ERS probe was equilibrated with the HBSS−25 mM HEPES buffer used for bioassays. The Millicell-ERS (Millipore) has two electrode-hands coated with silver pellets at the end of the probe-hands. Electrical current was measured from the apical side into the basolateral side. To validate measurements, TEERs of empty transwell inserts

(without cell monolayers) were determined using HBSS−25 mM HEPES, to correct the TEER calculations. TEERs were measured before and after bioassay. Values obtained were used, together with $^{14}$C-mannitol transport to monitor cell monolayer qualities.

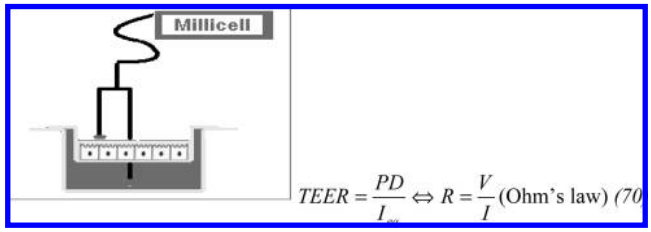


PD is potential differences between the transwell insert and the chamber bottom; $I_{eq}$ is equivalent short-circuit current, $I$ is electrical current, $V$ is voltage, and $R$ is resistance. Monolayer TEER measurement is the Milli-Cell reading in kΩ.

$$\text{monolayer TEER (k}\Omega\text{.cm}^2) = [R_{(\text{monolayers})} - R_{(\text{membrane support})}] \times A_{\text{transwell insert}}$$

*Bioassay.* Apical digest samples were supernatants obtained from digested samples after centrifugation at 4400 rpm and 10 °C for 15 min obtained from Nutriomic Analysis Part 1. Basolateral solution samples were buffer HBSS containing 25 mM HEPES at pH 7.4 used as a biological buffer system. The buffer mostly contains glucose and minerals.

The bioassay method used is a modified version of that reported by Blanchfield et al. (*71*). Experiments were carried out in an incubator (Heidolph Titramax 1000 shaker with a high hood, John Morris) at 350 rpm and a temperature of 37 °C, with 450 μM sample solutions to obtain measurable levels of various metabolites. Apical solutions (200 μL) were applied to the apical sides of the transwell inserts, and 600 μL of HBSS−25 mM HEPES was added into the basolateral compartments. Sampling regimens were 400 μL from the basolateral solutions every 30 min for the transit chyme model (**model A**) and the semidynamic model (**model B**); in addition, for the transit methods, the apical sides were emptied (for analysis) and a fresh apical solution (200 μL) was added every 30 min, whereas after 120 min of bioassay, 175 μL of the apical solution in semidynamic method was sampled. Permeability was calculated from model B. The monolayers had a passage number of either 64−65 or 28−36. Each sample had two transwell insert replications for each type of digesta.

Permeability is a value indicating how quickly the target compounds cross the epithelial cells regardless of whether by transcellular or paracellular pathways. It is assumed that passive diffusion predominantly takes place according to Fick's law. Permeability is calculated on the basis of simple diffusion rates of compounds penetrating the epithelial cell membranes. Experiments were validated with permeability values of reference compounds, that is, caffeine (100%), atenolol (50%), and $^{14}$C-mannitol (15%), determined from four transwell inserts for each compound.

$$P_{\text{app}} = \frac{\mathrm{d}C}{\mathrm{d}t} \times \frac{V_{\text{r}}}{AC_0}$$

(d$C$)/(d$t$) = steady-state rate of change in the radiochemical for mannitol or molecular concentration (dpm mL$^{-1}$ for mannitol; μM for other compounds) in the receiver chambers; $V_{\text{r}}$ = the volume of aliquot obtained from the receiver chambers; $A$ = the surface area of the cell monolayers − surface area of transwell insert bottom (24 wells have 6.5 mm membrane diameters); and $C_0$ = the initial concentration of the donor chamber (dpm mL$^{-1}$ s$^{-1}$ or μM).

*Chemical Analysis.* Sample preparations were carried out according to **Scheme 1** in the Nutriomic Analysis Part 1. The 1 mL cartridges were used during sample preparations.

*Carotenoid Analysis.* After filtration using a 0.22 μm nylon filter, the samples were eluted in a UPLC system (Waters Aquity model F06UPD365M) with a PDA detector. UPLC gradient composition of

**Scheme 1.** Bioassay Protocol

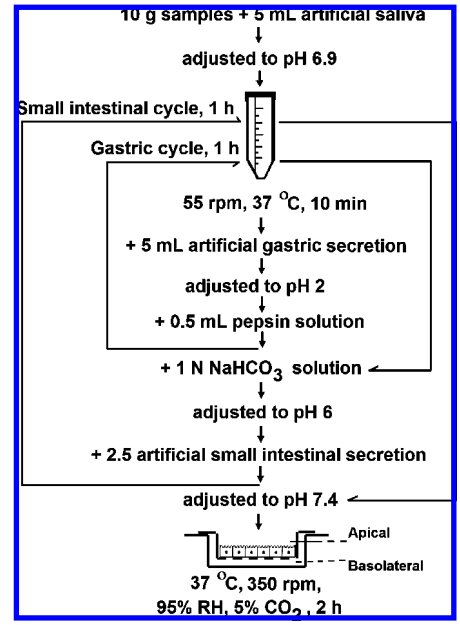


acetonitrile containing 0.1% formic acid (A) and MTBE (B) was 2.5% B for 0.1 min, increased to 7.5% using slow increment gradient for 0.3 min, 10% for 0.1 min, 12.5% for 1 min, and returned to 2.5% for 1.5 min using a sudden increased gradient to washed and equilibrate the column before the next injection.

A flow rate of 0.45 μL/min through a $C_{18}$ BEH column, which is a Bridged Ethanes in Hybrid matrix column [50 × 2.1 mm with packing material consisting of 1.7 μm particles with a pore size 80−125 Å (Waters)], was applied.

Chloroform extracts were dried under a nitrogen gas stream, reconstituted in 50% MTBE−methanol for maximum carotenoid solubility, and sonicated for 1 min. This solvent base is too strong for the UPLC system (personal communications, Waters); however, it dissolved carotenoid mixtures the best. MTBE <50% poorly dissolved lycopene and higher proportions of MTBE degraded lutein. To compensate, weak wash solvent after the 50% MTBE was 90% methanol−water containing 0.1% formic acid, and strong wash solution was 100% methanol. Samples were filtered through a 0.22 μm nylon filter prior to injection.

*Phenolic Analysis.* A Waters Acquity UPLC system model F06UPD365 M with a photodiode array (PDA) detector was used. The UPLC mobile phase involved two solvent mixtures: A, acetonitrile containing 0.1% formic acid; and B, Milli-Q filtered water containing 0.1% formic acid. The UPLC gradient was as follows: 5% B at the start, 40% B for 1 min with a linear increment gradient, 73% B for the next 2 min, 10% B for 1 min, and return to 5% before the next injection. A $C_{18}$ BEH column (50 × 2.1 mm using packing material with 80−125 Å pore size of 1.7 μm particles) was used at a flow rate of 0.45 mL/min.

*Sugars HPLC-ELSD and organic acids and vitamin C HPLC-UV methods* were similar those given in the first paper on nutriomic analysis of fresh and processed fruit products. Modification is for SPE cartridges: 1 mL instead of 3 mL. Additional validated standard compounds were lycopene and β-carotene in HBSS (100%).

*Calculating Potential Bioavailability of Sugars.* The cumulative transported sugars through an effective monolayer area of 0.33 cm$^2$ over 2.5 h, from bioassay samples of 1 mL, is $C_{\text{Bs}}$ nmol. The delivery rate of sugars across the cell monolayers ($D$) was calculated as

$$D = C_{\text{Bs}}\,(\text{nmol})/(0.33\ \text{cm}^2 \times 2.5\ \text{h}) = D \times 10^{-6}\ \text{mmol cm}^{-2}\ \text{h}^{-1}\ \text{mL}^{-1}$$

Glucose (MW = 180 g mol$^{-1}$) in total volume of digest $V$ (mL) obtained from initial weight of samples $W$ (g) with moisture content of $M_{\text{c}}$ (%) producing the potential bioavailability (BI) of the total sugars as glucose equivalent can be calculated as

$$\text{BI (g cm}^{-2}\text{ h}^{-1})/100\text{ g (WB)} = D \times 10^{-6}\text{ (mmol cm}^{-2}\text{ h}^{-1}\text{ mL}^{-1}) \times \frac{\text{V (mL)} \times 180\text{ (mg mmol}^{-1})}{W\text{ (g)}} \times 100$$

*Calculating Sugar Bioavailability.* An approximate surface area of 200 $m^2$ was estimated from the jejunum surface area of 184 $m^2$ (*72*) as the effective absorption area for various compounds in food. However, the sugar amounts from 100 g samples were too little to be spread over 200 $m^2$ absorptive areas. Effective area ($A$) at 1 h after a meal was calculated as

$$A\text{ (cm}^2) = \frac{C_1\text{ (g)}}{\text{BI (g cm}^{-2}\text{ h}^{-1}) \times 1\text{ h}}$$

Meanwhile, in an hour in healthy adult human continuously circulated 72 beats/min × 65 mL of blood/beat × 60 min = 280.8 L. When physical activity is high, the glucose is used up by the cell from the circulated blood. This is called the lower limit (LL). When the blood glucose is not rapidly used in the body, it accumulates in the total volume of human blood of 5 L after 1 h of absorption. This is called the upper limit (UL). Assuming the levels of absorbed sugars from the ingested foods were similar to that obtained from Caco-2 bioassays

$$\text{LL} = C_1\text{ (g h}^{-1})/280000\text{ mL} = \text{L mg h}^{-1}\text{ mL}^{-1}\text{ whole blood}$$

$$\text{UL} = C_1\text{ (g h}^{-1})/5000\text{ mL} = \text{L mg h}^{-1}\text{ mL}^{-1}\text{ whole blood}$$

## RESULTS AND DISCUSSION

**Validation.** Caco-2 cell monolayers, collected originally from a human colon cancer, were used for this in vitro simulation. Caco-2 cells express various physiological characteristics and have transporters similar to those in the human intestine when the cells differentiate completely (*73*, *74*). Thus, the choice is acceptable even though there may exist principal physiological rates compared to normal cells.

Validation with reference compounds produced higher permeability values, $P_{app}$, and slightly higher in vitro percentages of translocated compounds compared with the reported literature values (**Table 1**) but still acceptable, for example, caffeine (105.81 vs 100%), atenolol (68.48 vs 50%), and $^{14}$C-mannitol (2.21 vs 15%). This validation methods applied bioassay model B similar to methods generally used in permeability study of drugs in pharmacology for which in vivo data are available.

$P_{app}$ values of atenolol and caffeine were 25−40 and 2−3 times, respectively, higher than literature data, at least partly because apical solution concentrations were 2.5 times the concentration usually used in the pharmaceutical literature (where data comparing Caco-2 cell $P_{app}$ values to in vivo bioavailabilities are available for reference compounds), and the volumes applied were twice as high. Mass transfer was unaffected by the different concentrations and volumes of the apical solutions applied, but the $P_{app}$ was affected. Therefore, any comparisons of permeability values, $P_{app}$ require interpretation with caution, and the details of bioassay conditions should always be provided (e.g., TEER, volume, and concentration). This suggests that the assumption of passive diffusion may need to be re-evaluated and accommodate variation in cancerous cells.

TEER measurements are more practical, quick, and easy compared to the mannitol permeability values for assessing the integrity of tight junctions. Monolayers can be omitted immediately when TEER values before a bioassay are lower than the minimum limit.

The quality of the monolayers was checked. In the present study, all digest solutions that were subjected to bioassay using Caco-2 cell monolayers and renewed every 30 min (model A) resulted in the TEER values listed in **Table 2**. The initial TEER values of the monolayers ranged from 0.429 to 0.541 kΩ.$cm^2$. TEER values of 0.35−0.75 kΩ/$cm^2$ were used in experiments using dimers, trimers, and polymers of proanthocyanidin (*79*) and 0.250 kΩ/$cm^2$ was used for tea polyphenols (*16*). Commonly accepted TEER values for bioassays are >400 Ω/$cm^2$ (*71*), which is equivalent to >0.04356 kΩ.$cm^2$ (unit preferred and to be used further) or reading in Millicell-ERS >0.132 kΩ. TEER was calculated according to the equation in the aforesaid method. The TEER values show that the monolayers used in the present research had a high integrity and were therefore in good condition to act as a model for intestinal epithelia.

A preliminary study of the above bioassays showed that dried digests (water removed), when reconstituted in HBSS-25 mM HEPES buffer to achieve 200 μM concentrations, killed the cells and caused the monolayers to detach from the membrane support. This confirmed that tight junction integrity is sensitive to ions, including bile components, even though tight junctions are highly selective toward molecules transported by the paracellular route. Therefore, the concentration of the digest contents is critical for monolayer integrity. However, ratios of 1:10 for dry solid/gastrointestinal juices based on data on average fruit consumption by Australians were seen as realistic.

Generally, lowered TEER values were obtained from bioactive compounds and mannitol only after long (4 and 22 h) bioassays. Hence, up to 450 μM of a single bioactive compound in contact with the monolayers for a short time was nontoxic toward the Caco-2 cells. Thus, a 2 h bioassay was established, noting that an estimation of the transit time along the human small intestine is 2−6 h (*80*).

HBSS−25 mM HEPES buffer solution was subjected to Caco-2 monolayers for bioassay using a transit model, to establish baseline changes in glucose levels that occur during bioassay, because glucose is consumed by physiologically active Caco-2 cells. The absolute amounts (nmol) of apical glucose ($C_{Ap}$) were lower than that for the basolateral compartment because the buffer was applied to apical sides in 200 μL volumes, whereas basolateral volumes were 600 μL. During experiments, HBSS−25 mM HEPES solutions did not reduce TEER values of the monolayers to the values <0.200 kΩ.$cm^2$, showing that buffer alone does not affect the viability of the cells.

A point of difference in this method from the real human intestine system is that the chyme moves along the lumen, whereas in the model the apical solutions are static for 30 min. Also, possible variations may be due to cancerous cell physiology. Generally, previously published studies using Caco-2 monolayers did not measure TEER values, and comparison is not possible. Whether the phenomena-reduced TEER due to fruit digests translate into an in vivo degradation of gut epithelial cells by concentrated extracts from fruits remains to be seen, but is worthy of further study.

**Nutriomic from Tomato.** During bioassay, carotenoids present in the digest solutions of tomato products were found to completely disappear from the apical solutions. In response to this finding, fruit digests in each apical were spiked with β-carotene (8.8 μg/μL) for another batch of bioassay: here, approximately 100% of the spiked β-carotene was recovered from the apical samples at time 0 min (prepared apical solution

**Table 1.** Comparison of $P_{app}$ Values with Literature Values for Method Validation

| | present study | | | |
|---|---|---|---|---|
| | TEER (kΩ.cm$^2$) | | | |
| compound | before | after | $P_{app}$ (nm/s) | $P_{app}$ literature (nm/s) |
| $^{14}$C-mannitol | 0.3894 | 0.165 | 73.27 ± 2.84[a] [2.21%][d] | from 23 ± 2 to 32 ± 5 (15%) (*75*)[c] 58.8 ± 8.7 (*71*)[c] 18 (*76*)[c] 8 (*77*)[c] |
| | 0.4785 | 0.08745 | 41 ± 0.527[b] | 17 (16%) (*78*)[c] |
| atenolol | 0.5371 | 0.4554 | (1.46 ± 0.16)E3 [68.48%] | from 25 ± 4 to 40 ± 6 (50%)(*75*)[c] 200 (*76*)[c] 28 (50%) (*78*)[c] |
| caffeine | 0.4915 | 0.41745 | (1.92 ± 0.008)E3 [105.81%] | from 331 ± 27 to 410 ± 33(*75*)[c] (100%) |

[a] $^{14}$C-Mannitol, 200 μL. [b] $^{14}$C-Mannitol, 100 μL. [c] Using a Caco-2 clone TC7. [d] Values in parentheses are in vivo data and those in brackets are % in vitro after 120 min compared to initial concentration at 0 min.

**Table 2.** TEER Values of Bioassay Using Digest Solutions of Fruit Products (Entries in Bold Represent Unacceptably Low TEER Values for Monolayer Integrity)

| sample | TEER before (kΩ.cm$^2$) | TEER after (kΩ.cm$^2$) |
|---|---|---|
| tomato juice | 0.454 | **0.136** |
| dried tomato | 0.437 | **0.084** |
| tomato fresh | 0.429 | 0.256 |
| mango juice | 0.536 | **0.130** |
| dried mango | 0.533 | **0.160** |
| mango fresh | 0.490 | 0.376 |
| papaya juice | 0.541 | 0.375 |
| dried papaya | 0.409 | **0.124** |
| papaya fresh | 0.526 | 0.254 |

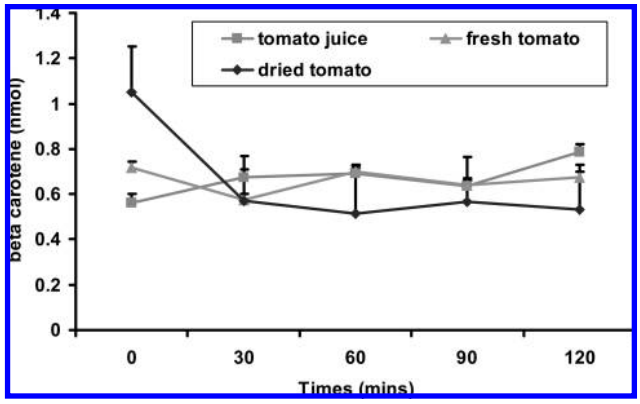


**Figure 1.** Apical changes (spiked tomato digests with β-carotene) using model A, using two wells for each product.

composed of the spiked tomato digests) (**Figure 1**), and no basolateral β-carotene was found. In addition, there was no evidence for any passage of β-carotene in this system studied over 120 min of bioassay. Thus, it is suggested that minor components in the fruit digests may be the cause for the nonabsorption of β-carotene besides the lack of lipid to help solubilization. It is speculated that β-carotene was bound to pectin in the tomato digest solution without sufficient dietary lipid, making it retained in the apical solutions, than when prepared as pure solution in the HBSS−25 mM HEPES buffer. Bound carotenoids are possible as dietary fiber can modulate physiological conditions of mucosal environment of the intestine (*81, 82*). The animal in vivo using gerbils showed that citrus pectin inhibited the absorption and conversion of β-carotene which has been consistently proven in in vivo human and chicken studies, specifically when high molecular weight and

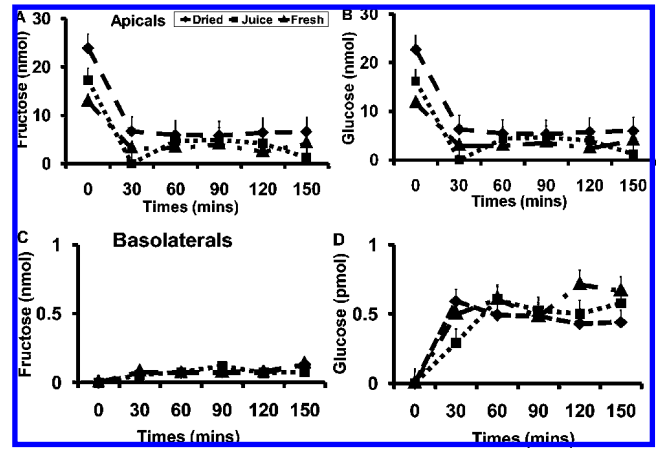


**Figure 2.** Sugars uptake and transport from tomato digests by Caco-2 cell monolayers using the transit model (model A).

high-methoxylated pectin is present (*83*). Generally, fruits contain high-methoxylated pectin. This warrants that an increase of fruit consumption without sufficient dietary lipid causes bound carotenoids to go to the large intestine.

Retinol-like compounds were irreproducibly obtained from the Caco-2 bioassays at very low levels in this research when pure β-carotene apical solutions were applied. Although this shows that it is possible for Caco-2 cells to metabolize carotenoids, the lack of reproducibility makes it difficult to draw definitive conclusions. Partly, this can be due to Caco-2 unstable β-oxidase expression and cancerous cells. Studies of carotenoid bioavailability in pectin-rich fruits have not been done before. Analysis of the results in the present study indicates that pectin may disturb carotenoid absorption/metabolism by gut epithelial. In the real human system, this probably leads to carotenoid transport to the colon, where uptake and/or microbial metabolism may take place. It is therefore concluded that the responses of Caco-2 cell monolayers to carotenoids in digest solutions are likely to be significantly affected by the presence of pectin when insufficient dietary lipid occurs.

Sugars were not retained by pectins and can be transported into the basolateral sides in Caco-2 cell assays without particular selectivity; thus, fructose, glucose, and sucrose were translocated into the basolateral sides from fruit digests (**Figure 2**). The disappearance of sugars from the apical sides, again similar to other compounds, was not equal to those secreted in basolateral sides.

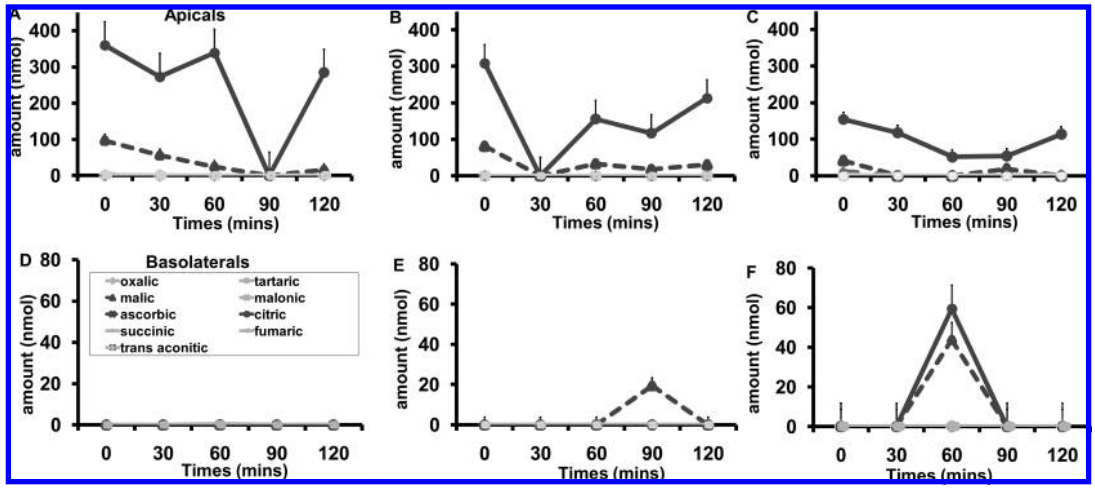


**Figure 3.** Uptake and transport of organic acids from tomato digests by Caco-2 monolayers using the transit model (model A): dried tomato (**A**, **D**), tomato juice (**B**, **E**); fresh tomato (**C**, **F**); **A**−**C**, apical; **D**−**F**, basolateral.

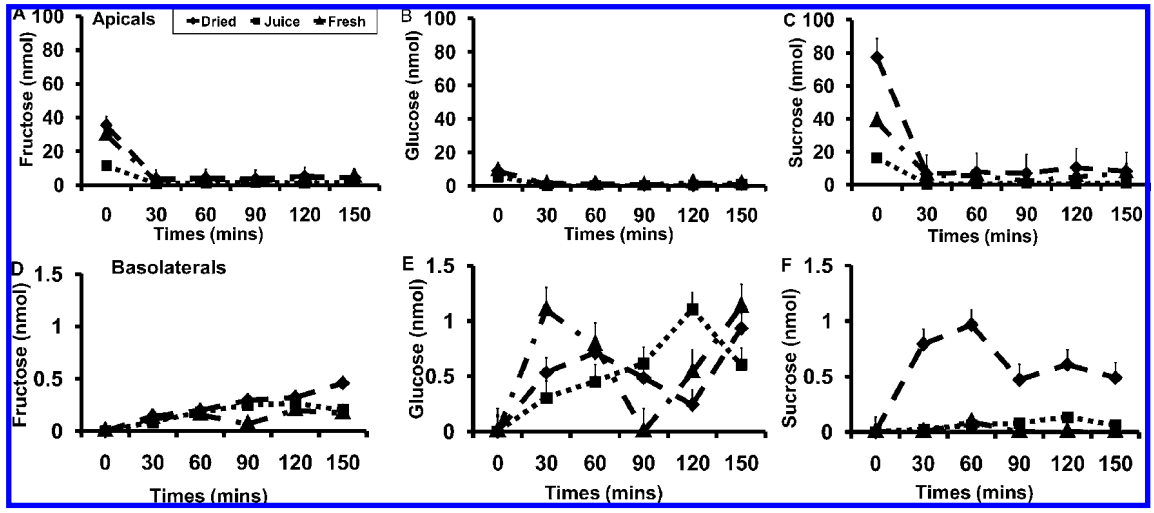


**Figure 4.** Sugar uptake and transport from mango digest solutions by Caco-2 monolayers using transit model (model A): (**A**,**D**) fructose; (**B**,**E**) glucose; (**C**,**F**) sucrose; **A**–**C**, apical; **D**–**F**, basolateral.

After correction for buffer glucose contents, it was found that only 2.5−6% of the initial glucose content from the digest solutions was transported into the basolateral side. A smaller amount of fructose (0.4−0.7%) was also transported, although its rate of disappearance from the apical sides was similar to that of glucose. Fructose and glucose enter glycolysis pathways in cytoplasm as fructose-1P or fructose-6P and glucose-6P, respectively; thus, the high losses may be due to their status as energy sources for the Caco-2 cells. Currently, it is not understood how Caco-2 cells control the amount of sugars to be translocated into the basolateral, along with the amount for cell metabolism ($Na^+$−$Ka^+$ATPase requires high energy to operate) (*84*).

Additionally, there was no relationship between measured TEER values and the translocated amounts of sugars. Tomato juice, for which the TEER values dropped to 0.13 $k\Omega.cm^2$, did not translocate higher amounts of glucose. The recorded translocation amounts suggest only small amounts of sugars were not used for metabolism by the cells or, alternatively, that the Caco-2 cell monolayer pores are smaller than the size of the glucose molecule. Hidalgo (*74*) recorded that the sizes of the pore or tight junctions in human intestinal cell layers are approximately 4−8 Å, which is in the same size range as for a hydrated sugar molecule. This provides further evidence that the cell monolayers do not act as a physical barrier to sugar absorption and that Caco-2 cells use the sugars in tomato digests for energy. As it is unlikely that dietary sugars provide fuel for intestinal epithelia in vivo, the proposal that relatively low transport of sugars in the Caco-2 cell assay is due to metabolism means that any extrapolation to the in vivo situation will likely underestimate real transported amounts.

The released acids were subjected to Caco-2 monolayers (**Figure 3**). The dominant organic acids, citric acid and malic acid, were detectable from the 200 $\mu$L digest solutions, whereas the minor acids were not. Continual supply of digest solutions did not show accumulation of citric or malic acids. In the basolateral compartments, malic and citric acids were detected sporadically at 60 or 90 min. When observed, the basolateral acids were 2−20% of the acids detected in the apical solutions at 0 min.

During Caco-2 bioassays neither basolateral nor apical phenolics appearances were found. This suggests the uptake of phenolics from the digests by the Caco-2 cells and subsequent metabolism. Metabolites at minute levels may be undetectable in this study.

**Nutriomic from Mango.** Bioassay results for sugars are presented in **Figure 4**. General disappearances of sugars from apical sides followed trends found for various other target compounds. Phenomena of nutriome disappearances consistent with those from tomato products were obtained.

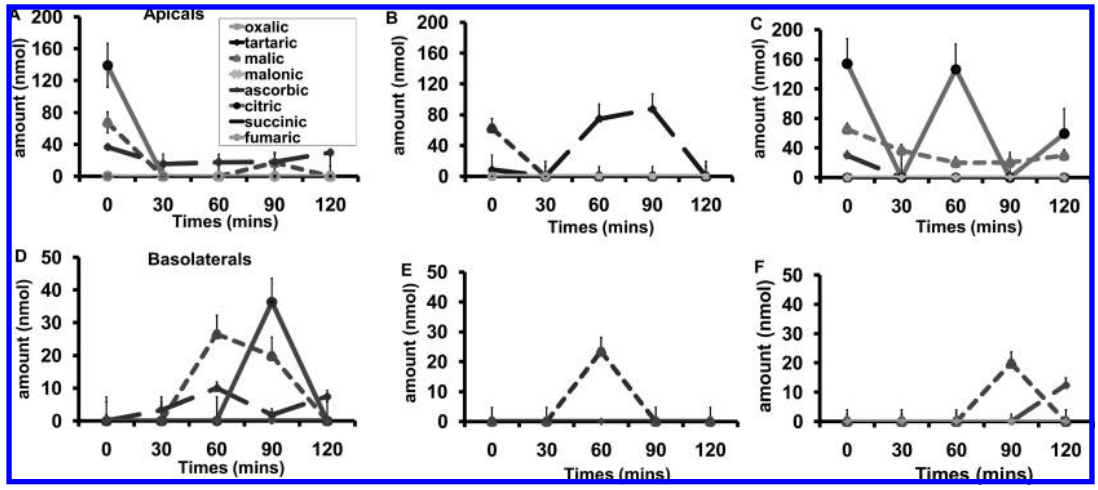


**Figure 5.** Uptake and transport of organic acids from mango digest solutions in Caco-2 monolayers (model A): (top row, apicals; bottom row, basolaterals) (**A**, **D**) dried mango; (**B**, **E**) mango juice; (**C**, **F**) fresh mango.

For all mango products, the level of fructose in the basolateral side steadily increased to relatively similar levels. This suggests there is no particular effect of the source of fructose on absorption by the Caco-2 monolayers. However, sucrose and glucose were transported at higher levels than fructose. Their translocation profiles fluctuated and were different for each source of sugar. All mango products showed fluctuating glucose transport, whereas sucrose transport increased. Sucrose disappearance from dried mango was the highest and synchronized with the highest amount of sucrose found in the basolateral side compared to other products. Basolateral sucrose from fresh mango reached a peak at 60 min, whereas fructose steadily increased and leveled off at 150 min.

On the other hand, the glucose content of mango products was low, and the transports for each product were quite similar. Basolateral glucose from fresh mango peaked earlier at 30 min, then reached a minimum at 90 min, and finally increased again until 150 min. Similar fluctuations occurred for dried mango, but the times were decreased by 30 min. The basolateral glucose transported from mango juice digests steadily increased and peaked at 120 min, the same time as dried mango, but it decreased thereafter, whereas basolateral glucose from dried mango digests increased thereafter.

During in vitro absorption by Caco-2 cell monolayers, each acid showed a different behavior (**Figure 5**). In the digests from dried mango, ascorbic, citric, and malic acids were found in the basolateral side. Small amounts of loss of ascorbic acid from the apical side were coupled with its secretion in basolateral side, indicating that ascorbic acid was not metabolized and was secreted intact into the basolateral compartment by the Caco-2 monolayers. Malic acid was secreted into the basolateral side, with its maximum concentration being at 60 min, after which its concentration declined continuously until 120 min, whereas citric acid reached its maximum concentration in the basolateral side at 90 min.

However, this was not consistent with what happened for the mango juice. Malic acid disappeared from the mango juice digests in the apical side during the first 30 min, with it being secreted into the basolateral side, finally reaching a maximum concentration at 60 min. In contrast, ascorbic acid was retained and accumulated in the apical side and decreased to zero at 120 min without basolateral secretion. Further inconsistency was observed for the fresh mango, where citric acid fluctuated when continuous digest solutions were supplied as part of this bioassay model. This effect was different from that observed for malic

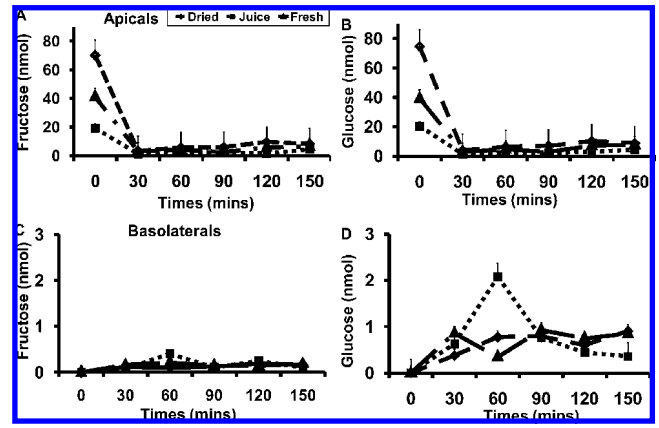


**Figure 6.** Sugars uptake and transport by Caco-2 monolayers from papaya digest using transit chyme model (model A; using two transwell inserts).

acid, which gradually decreased (**Figure 6C**) in a pattern similar to that observed for ascorbic acid from dried mango digests (**Figure 6A**). Ascorbic acid from fresh mango digest had disappeared from the apical side by 30 min; further 30 min replacements of the apical solution with fresh mango digest did not result in ascorbic acid being observed in the basolateral solutions at 90 min. Although all monolayers had acceptable TEER values, the high level of variability in the behavior of similar molecules or the same molecules from different mango product sources requires further investigation. Being sure of the uniformity of the Caco-2 cell monolayers definitely requires serious attention before results can be interpreted with confidence from such a study.

**Nutriomic from Papaya.** Similar to other carotenoid bioassays of the fruit digest solutions, there were not found any carotenoids in apical and basolateral compartment. Thus, the samples were spiked with 22 $\mu$g of $\beta$-carotene each. The spiking of the samples with $\beta$-carotene indicated the possible role of pectic substances; because of the spike, $\beta$-carotene could be found in the apical side but not in the basolateral side. On the other hand, a preliminary experiment using pure $\beta$-carotene showed the $\beta$-carotene partially disappeared from the apical side. Hence, the finding suggested that digest solution containing cell wall material caused $\beta$-carotene to be retained in the apical side. Further study needs to be carried out.

Bioassays of digest solutions of papaya products using model A showed high apical decreases for all sugar types; sugars

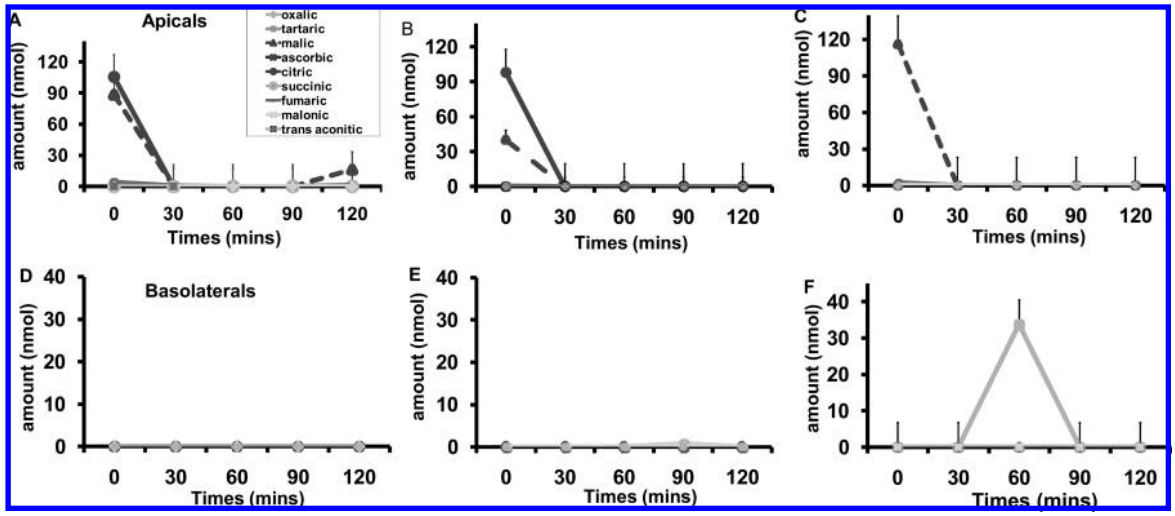


**Figure 7.** Organic acids uptake and transport in Caco-2 monolayers (model A; using two transwell inserts): (**A**, **D**) dried papaya; (**B**, **E**) papaya juice; (**C**, **F**) fresh papaya.

**Table 3.** Sugar Potential Bioavailability from Tomato Products Expressed as Glucose Equivalent

| sample | potential glucose bioavailability ($g \cdot cm^{-2}\ h^{-1}$) WB | glucose delivery rate (g/h) WB | mg $h^{-1}$ $mL^{-1}$ whole blood | |
|---|---|---|---|---|
| | | | LL | UL |
| dried tomato | 0.000867 (49.78%)[a] | 27.135 | 0.097[b] | 5.427[c] |
| tomato juice | 0.000128 (100%)[a] | 3.909 | 0.014[b] | 0.782[c] |
| fresh tomato | 0.000124 (89.45%)[a] | 2.27 | 0.008[b] | 0.454[c] |

[a] Comparison in % (DB) to juice. [b] Assumed that glucose is rapidly used in the body in 1 h circulated blood (280 L). [c] Assumed that glucose is deposited in the total blood (5 L) for 1 h after a meal.

secreted into the basolateral compartments were only 0.7−1.4% of the original apical concentration, which is consistent with metabolism by Caco-2 cells being the dominant process. Glucose was lost from the apical compartment over the first 30 min, and transport increased over time, reaching an apparent stationary phase at 60 min. Similar results were found for fructose but at lower levels than for glucose.

Caco-2 monolayers transported organic acids (**Figure 7**). Generally, organic acids disappeared from the apical compartments; however, they were seldom found in the basolateral solutions, and then only at very low levels. Addition of further digest solutions to the apical side did not affect the responses, and apical accumulation of organic acids was not observed. These data suggest that organic acids in papaya are metabolically consumed very efficiently by the cells. Organic acids found in both human plasma and food materials include lactic, citric, galacturonic, and *o*-hydroxycinnamic acids (*85*). Several additional organic acids were found in diabetic patients, such as fumaric and glutaric. These authors reported the citric acid levels in the plasma of diabetic patients were double those in healthy human plasma. However, it is unexplained whether those acids were obtained from dietary intake or (more likely) were due to metabolism. The organic acids produced during metabolism are disposed off through renal reabsorption (*86*). Therefore, dietary organic acids may be absorbed into the circulatory system, as occasionally observed in this study, and are probably released in the urine.

Cellular uptake of ions is expected to be affected by the electrolyte concentration and pH of the apical solution. Among anions, there are interactions; for example, in renal epithelial cells, the presence of formate decreases oxalate uptake. Salovaara et al. (*87*) found the effect of citric and oxalic acids on iron uptake by Caco-2 cell monolayers involves formation of a complex between iron and anions of citric and oxalic acids and that any effect on the pH of the bioassay microenvironments depends on their concentration.

Caco-2 bioassays of the digest solutions resulted in no carotenoids in either the apical or basolateral sides for any digest. This indicated that phytochemicals are likely absorbed from the colon, not the small intestine, whereas glucose as an energy source is mainly absorbed in the small intestine. The disappearance of carotenoids from the apical side of the Caco-2 cell monolayers found in the present study (for all digest solution samples) is in agreement with ref *14*, in which the digestion did not use oil and the pure compounds were prepared in DMSO. In the present study, DMSO levels were controlled at 0.5−1%, which is lower than that in the referred experiments. Presumably, the phytochemical benefits are obtained from the colon involving microbial metabolisms.

In the study, when $\beta$-carotene was added to apical compartments, basolateral retinol-like compounds were occasionally detected, but not reproducibly produced by the Caco-2 cells. This demonstrates an element of variability in the way that individual Caco-2 cell monolayers behave. The results of in vivo studies (*1*, *2*) involving retinol formation from kale labeled nutrients and from in vitro studies using Caco-2 cell lines (*88*) were thus not fully replicated in the present research. It is important to investigate further the factors affecting Caco-2 cell regulation related to metabolism or translocations when a mixture of nutriome components is applied to apical compartments. Also, it is possible that the existence of phytochemicals is minor in the whole natural food system.

To sum up sugar transports, in vitro absorption studies of a mixture of nutriome in digest solutions of tomato, mango, and papaya products indicated that translocation of the predominant compounds into the basolateral compartments during bioassay was detectable (albeit often at low levels) and can be used for determination of the potential bioavailability of compounds. Juices have the highest potential bioavailability of sugars, as would be expected, supporting the idea to use 100% juice as a reference for nutritional high-density food products. Other

**Table 4.** Sugar Potential Bioavailability from Mango Products Expressed as Glucose Equivalent

| sample | potential glucose bioavailability ($g \cdot cm^{-2}\ h^{-1}$) WB | glucose delivery rate (g/h) WB | mg $h^{-1}$ $mL^{-1}$ whole blood | | reference mg $h^{-1}$ $mL^{-1}$ whole blood |
|---|---|---|---|---|---|
| | | | LL | UL | |
| dried mango | 0.00190 (56.78%)[a] | 75.98 | 0.270[b] | 15.196[c] | na[e] |
| mango juice | 0.000208 (100%)[a] | 7.39 | 0.024[b] | 1.478[c] | na |
| fresh mango | 0.000168 (22.81%)[a] | 2.26 | 0.008[b] | 0.452[c] | 0.288[d] |

[a] Comparison in % (DB) to juice. [b] Assumed that glucose is rapidly used in the body in 1 h circulated blood (280 L). [c] Assumed that glucose is deposited in the total blood (5 L) for 1 h after a meal. [d] Original data in vivo serum level after 1 h consumption of fresh mango in diabetic people 13.7 mmol/L with baseline glucose level of 9.7 mmol/L (*6*) recalculated for 280 L circulated blood for 1 h. [e] na, data not available.

**Table 5.** Potential Bioavailability of Sugars from Papaya Digests Determined in Vitro and Expressed as Glucose Equivalent

| sample | potential glucose bioavailability ($g \cdot cm^{-2}\ h^{-1}$) WB | glucose delivery rate (g/h) WB | mg $h^{-1}$ $mL^{-1}$ whole blood | | reference mg $\cdot h^{-1}$ $mL^{-1}$ whole blood |
|---|---|---|---|---|---|
| | | | LL | UL | |
| dried papaya | 0.000583 (18.656%)[a] | 34.142 | 0.122[b] | 6.828[c] | na[e] |
| papaya juice | 0.000225 (100%)[a] | 4.731 | 0.017[b] | 0.946[c] | na |
| fresh papaya | 0.000189 (36.656%)[a] | 5.573 | 0.020[b] | 1.115[c] | 0.152[d] |

[a] Comparison in % (DB) to juice. [b] Assumed that glucose is rapidly used in the body in 1 h circulated blood (280 L). [c] Assumed that glucose is deposited in the total blood (5 L) for 1 h after a meal. [d] Original data in vivo serum level after 1 h consumption of fresh papaya in diabetic people 14.3 mmol/L with glucose baseline of 9.2 mmol/L (*6*) recalculated for 280 L circulated blood for 1 h. [e] na, data not available.

products had 18.7−89.5% potential glucose bioavailability compared to their corresponding juices with the potential glucose levels of the order tomato (49.8% dried; 89.5% fresh) > mango (56.8% dried; 22.8% fresh) > papaya (18.7% dried; 36.7% fresh). This means that consumption of fruit juice supplies more glucose than consumption of the same amount of fresh or dried fruits, in addition to potential insulinemic responses in the human body. Potential sugar bioavailability expressed as glucose equivalent is listed in **Tables 3−5** and was calculated according to aforementioned equations in the methods. Clearly, the estimations did not indicate insulinemic compared to those observed in in vivo diabetic people (*6*) but close to normal limits after meals (100 mg/dL) (*89*).

In the present study, during bioassays, there were high sugar losses during transportation from the apical compartment to the basolateral compartment when measured as absolute amounts (nmol). The low levels of transported sugars were due to high losses resulting from metabolism of sugar by the Caco-2 cells, consistent with the fact that Caco-2 cells are cancerous cells. Cancer cells have extremely high metabolism and accumulate glycogen (*90*). In contrast, Fuse et al. (*91*) reported that in rats, glucose absorption decreased due to expansion of the unstirred-water layer in the presence of soluble pectin, in line with the findings of Schneeman and Gallaher (*81*) that pectin can interact with mucosal layers. Gel pectin has been putatively proposed to absorb sucrose (*92*); however, in the present study, low levels of fructose, glucose, and sucrose were found at basolateral compartments. However, attempts to confirm physicochemical aspects of in vitro sugar absorption and links with insulinemic responses are required because the in vitro model currently used to study sugar delivery was free from hormonal regulation involved in the in vivo system.

Phenolics were not found in basolateral or apical compartments after bioassays, in line with other studies of phenolics using Caco-2 cell monolayers, which showed no basolateral phenolics (*91*−*93*). These authors (*93*) also examined the affinity of phenolics for the membranes in the Caco-2 cell monolayers and concluded that the high cell membrane affinity of phenolics resulted in poor basolateral translocation; that is, phenolics were retained in the cell layer. Transport and membrane affinity were reported as functions of hydroxylation number and molecular configurations. This was supported by ref *17*, reporting that inhibitory effects were obtained from monohydroxylated phenolic derivatives, but not those from di- and trihydroxylated phenolics. Phenolics were also found to bind transport proteins (*94*, *95*). This binding is both an advantage and a disadvantage. An advantage is that being bound aids their transport in blood and prevents oxidation in the human body (*96*). On the other hand, Kaldas et al. (*95*) observed that the complexity of quercetin−human protein serum was affected by peroxidase activity and was treated as a toxic component and excreted by the human body before exerting its functions. Similar phenolic binding with saliva protein may also cause low availability of phenolics (*97*), more specifically, for those phenolics composed of >3 flavonol subunits (*98*). Thus, in the developed model, the use of artificial saliva containing casein as proline-rich protein may have played a role in generating low levels of phenolics during in vitro digestions.

However, this is in apparent contradiction with findings from human ileostomists, where quercetin aglycone, quercetin, and quercetin-3-rutinoside were absorbed in the small intestine when urine was examined (*99*). Walgren et al. (*100*) showed that the quercetin 4′-$\beta$-glucoside was transported by SGLT1, which suggested that the translocations were due to cotransport with sugars. Thus, there is unintentional transport of phenolics into the blood circulatory system.

Overall, this nutriomic analysis showed that Caco-2 cell monolayers controlled uptake of nutriome components from the apical sides and their secretion into basolateral sides. The pattern of apical disappearances of target compounds during bioassays suggested that there are control mechanisms of Caco-2 cells toward different compound groups exposed to them. This is consistent with what has been reported for pure compounds in this research.

Modulations of TEERs (as a marker for monolayer integrity) during bioassays were not always followed by increases in the basolateral levels of analytes, indicating that passive diffusion by the paracellular routes is unlikely to happen. Diffusion theory has frequently been found to be applicable in biological systems (*101*), but appears not to be the dominant mechanism here. The finding of quantitative basolateral recovery of caffeine and (partially) atenolol as reference compounds shows that Caco-2 cells are capable of transporting molecules from the apical chamber to the basolateral chamber. The fact that low basolateral concentrations were detected occasionally for fruit nutriome components that disappeared completely from the apical sides

suggests that one of two possible mechanisms is occurring: (1) Nutriome molecules are taken up and used as a source of metabolic energy by the Caco-2 cells with corresponding low transport to the basolateral chamber. This is proposed to be the main mechanism operating for sugars and simple organic acids (e.g., citric), which are part of the normal glycolysis pathway in animal cells, which is supported by the anomalous characteristics of cancerous cells. (2) Nutriome molecules complex with cellular components, particularly proteins. This is proposed to be the reason why very low (often undetectable) amounts of phenolic and carotenoid transport into the basolateral chamber. Possible sites of complexation/absorption include the cell extracellular matrix or membrane proteins.

Capillary action plays an important role in transfer phenomena in both biological and porous materials (*101*). Therefore, the physical structures of materials and cell membranes/monolayers are likely to be critical factors in bioavailability. In mango products, fibrous matrices and viscous mass and cells even in juices may have equivalent capillarity to bulk matrices; thus, there is no difference in sugar release due to processing. This is in contrast with papaya, which has a shrunken and compacted structure after drying and/or chewing. In addition, in dried tomato, even though it has higher moisture content than dried mango or papaya, the effects of processing on nutrient releases were significantly different, presumably due to reduced capillarity compared with the fresh fruit.

In conclusion, in vitro intestinal absorption and transport using Caco-2 monolayers is a potential model to study the human digestive system, which is not able to be carried out in vivo. Validation using complementary TEER and permeability values or internal standard caffeine is recommended because passive diffusion is unlikely to happen. Bioassay conditions have been identified in this study to achieve meaningful data. Depletion rates from the apical compartment may be a better measure of uptake than appearance in the basolateral chamber due to the possible metabolism or binding of nutriome components with the Caco-2 cell monolayer, whereas bioavailability index is expressed from basolateral levels. Further study on the effects of pectin in absorption is required to explore its ability to bind phytochemicals, leading to the transit of phytochemicals into the colon, which warrants studies of phytochemical metabolites generated by colon microorganisms.

## LITERATURE CITED


(1) Kurilich, A. C.; Britz, S. J.; Clevidence, B. A.; Novotny, J. A. Isotopic labeling and LC-APCI-MS quantification for investigating absorption of carotenoids and phylloquinone from kale (*Brassica oleracea*). *J. Agric. Food Chem.* **2003**, *51*, 4877–4883.

(2) Novotny, J. A.; Kurilich, A. C.; Britz, S. J.; Clevidence, B. A. Plasma appearance of labeled ($\beta$)-carotene, lutein, and retinol in humans after consumption of isotopically labeled kale. *J. Lipid Res.* **2005**, *46*, 1896–1903.

(3) Breithaupt, D. E.; Weller, P.; Wolters, M.; Hahn, A. Plasma response to a single dose of dietary $\beta$-cryptoxanthin esters from papaya (*Carica papaya* L.) or non-esterified $\beta$-cryptoxanthin in adult human subjects: a comparative study. *Br. J Nutr.* **2003**, *90*, 795–801.

(4) Vaidyanathan, J. B.; Walle, T. Transport and metabolism of the tea flavonoid (−)-epicatechin by the human instestinal cell line Caco-2. *Pharm. Res.* **2001**, *18*, 1420–1425.

(5) Vaidyanathan, J. B.; Walle, T. Glucuronidation and sulfatation of the tea flavonoids (−)-epicatechin by the human and rat enzymes. *Drug Metab. Dispos.* **2002**, *30*, 897–903.

(6) Fatema, K.; Ali, L.; Rahman, M. H.; Parvin, S.; Hassan, M. Z. Serum glucose and insulin response to mango and papaya in type 2 diabetic subjects. *Nutr. Res. (N.Y.)* **2003**, *23*, 9–14.

(7) Chitchumroonchokchai, C.; Schwartz, S. J.; Failla, M. L. Assessment of lutein bioavailability from meals and a supplement using simulated digestion and Caco-2 human intestinal cells. *J. Nutr.* **2004**, *134*, 2280–2286.

(8) During, A.; Albaugh, G.; Smith, J. C. Charactrization of $\beta$-carotene 15,15′-dioxygenase activity in TC7 clone of human intestinal cell line Caco-2. *Biochem. Biophys. Res. Commun.* **1998**, *249*, 467–474.

(9) During, A.; Hussain, M. M.; Morel, D. W.; Harrison, E. H. Carotenoid uptake and secretion by Caco-2 cells: $\beta$-carotene isomer selectivity and carotenoid interactions. *J. Lipid Res.* **2002**, *43*, 1086–1095.

(10) Ferruzzi, M. G.; Failla, M. L.; Schwartz, S. J. Assessment of degradation and intestinal cell uptake of carotenoids and chlorophyll derivatives from spinach puree using an in vitro digestion and Caco-2 human cell model. *J. Agric. Food Chem.* **2001**, *49*, 2082–2089.

(11) Ferruzzi, M. G.; Lumpkin, J. L. Digestive stability, micellarization, and uptake of $\beta$-carotene isomers by Caco-2 human intestinal cells. *J. Agric. Food Chem.* **2006**, *54*, 2780–2785.

(12) Garrett, D. A.; Failla, M. L.; Sarama, R. J. Estimation of carotenoid bioavailability from fresh stir-fried vegetables using an in vitro digestion/Caco-2 cell culture model. *J. Nutr. Biochem.* **2000**, *11*, 574–580.

(13) Garrett, D. A.; Failla, M. L.; Sarama, R. J.; Craft, N. Accumulation and retention of micellar $\beta$-carotene and lutein by Caco-2 human intestinal cells. *J. Nutr. Biochem.* **1999**, *10*, 573–581.

(14) Liu, C.-S.; Glahn, R. P.; Liu, R. H. Assessment of carotenoid bioavailability of whole foods using a Caco-2 cell cullture model coupled with in-vitro digestion. *J. Agric. Food Chem.* **2004**, *52*, 4330–4337.

(15) Sugawara, T.; Kushiro, M.; Zhang, H.; Nara, E.; Ono, H.; Nagao, A. Lysophosphatidylcholine enhances carotenoid uptake from mixed micelles by Caco-2 human intestinal cells. *J. Nutr.* **2001**, *131*, 2921–2927.

(16) Konishi, Y.; Kobayashi, S.; Shimizu, M. Tea polyhenols inhibit the transport of dietary phenolic acids mediated by the monocarboxyclic acid transporters (MCT) in intestinal Caco-2 cell monolayers. *J. Agric. Food Chem.* **2003**, *51*, 7296–7302.

(17) Konishi, Y.; Kubo, K.; Shimizu, M. Structural effects of phenolic acids on the transepithelial transport of fluorescein in Caco-2 cell monolayers. *Biosci., Biotechnol., Biochem.* **2003**, *67*, 2014–2017.

(18) Konishi, Y.; Shimizu, M. Transepithelial transport of ferulic acid by monocarboxylic acid transporter in Caco-2 cell monolayers. *Biosci., Biotechnol., Biochem.* **2003**, *67*, 856–862.

(19) Laurent, C.; Besancon, P.; Caporiccio, B. Ethanol and polyphenolic free wine matrix stimulate the differentiation of human intestinal Caco-2 cells. Influence of their association with a procyanidin-rich grape seed extract. *J. Agric. Food Chem.* **2005**, *53*, 5541–5548.

(20) Lee, J. K.; Gordon, P. R.; Stall, G. M.; Gilchrest, B. A.; Kaplan, M. M. Phenolic and tyrosyl ring iodothyronine deiodination by the Caco-2 human colon carcinoma cell line. *Metabolism* **1989**, *38*, 1154–1161.

(21) Pal, S.; Ho, S. S.; Takechi, R. Red wine polyphenolics suppress the secretion of ApoB48 from human intestinal CaCo-2 cells. *J. Agric. Food Chem.* **2005**, *53*, 2767–2772.

(22) Roques, S. C.; Landrault, N.; Teissedre, P. L.; Laurent, C.; Besancon, P.; Rouane, J. M.; Caporiccio, B. Hydrogen peroxide generation in Caco-2 cell culture medium by addition of phenolic compounds: effect of ascorbic acid. *Free Radical Res.* **2002**, *36*, 593–599.

(23) Yun, S. M.; Habicht, J. P.; Miller, D. D.; Glahn, R. P. An in vitro digestion/Caco-2 cell culture system accurately predicts the effects of ascorbic acid and polyphenolic compounds on iron bioavailability in humans. *J. Nutr.* **2004**, *134*, 2717–2721.

(24) Au, A. P.; Reddy, M. B. Caco-2 cells can be used to assess human iron bioavailability from a semipurified meal. *J. Nutr.* **2000**, *130*, 1329–1334.

(25) Etcheverry, P.; Miller, D. D.; Glahn, R. P. A low-molecular-weight factor in human milk whey promotes iron uptake by Caco-2 cells. *J. Nutr.* **2004**, *134*, 93.
(26) Garcia-Casal, M. N.; Leets, I.; Layrisse, M. Ethylenediaminetetraacetic acid (EDTA) does not increase iron uptake or ferritin synthesis by Caco-2 cells. *J. Nutr. Biochem.* **2004**, *15*, 261–266.
(27) Glahn, R. P.; Wien, E. M.; van Campen, D. R.; Miller, D. D. Caco-2 cell iron uptake from meat and casein digests parallels in vivo studies: use of a novel in vitro method for rapid estimation of iron bioavailability. *J. Nutr.* **1996**, *126*, 332–339.
(28) Glahn, R. P.; Lai, C.; Hsu, J.; Thompson, J. F. Decreased citrate improves iron availability from infant formula: application of an in vitro digestion/Caco-2 cell culture model. *J. Nutr.* **1998a**, *128*, 257.
(29) Glahn, R. P.; Lee, O. A.; Yeung, A.; Goldman, M. I.; Miller, D. D. Caco-2 cell ferritin formation predicts nonradiolabeled food iron availability in an in vitro digestion/Caco-2 cell culture model. *J. Nutr.* **1998**, *128*, 1555–1561.
(30) Glahn, R. P.; Rassier, M.; Goldman, M. I.; Lee, O. A.; Cha, J. A comparison of iron availability from commercial iron preparations using an in vitro digestion/Caco-2 cell culture model. *J. Nutr. Biochem.* **2000**, *11*, 62–68.
(31) Glahn, R. P.; Cheng, Z.; Welch, R. M.; Gregorio, G. B. Comparison of iron biaovailability from 15 rice genotypes: studies using an in vitro digestion/Caco-2 cell culture model. *J. Agric. Food Chem.* **2002**, *50*, 3586–3591.
(32) Glahn, R. P.; Wortley, G. M.; South, P. K.; Miller, D. D. Inhibition of iron uptake by phytic acid, tannic acid, and $ZnCl_2$: studies using an in vitro digestion/Caco-2 cell model. *J. Agric. Food Chem.* **2002**, *50*, 390–395.
(33) Halleux, C.; Schneider, Y. J. Iron absorption by Caco 2 cells cultivated in serum-free medium as in vitro model of the human intestinal epithelial barrier. *J. Cell Physiol.* **1994**, *158*, 17–28.
(34) Han, O.; Failla, M. L.; Hill, A. D.; Morris, E. R.; Smith, J. C. Ascorbate offsets the inhibitory effect of inositol phosphates on iron uptake and transport by Caco-2 cells. *Proc. Soc. Exp. Biol. Med.* **1995**, *210*, 50–56.
(35) Han, O.; Failla, M. L.; Smith, J. C. Transferrin−iron and proinflammatory cytokines influence iron status and apical iron transport efficiency of Caco-2 intestinal cell line. *J. Nutr. Biochem.* **1997**, *8*, 585–591.
(36) Ho, S. Y.; Storch, J. Common mechanisms of monoacylglycerol and fatty acid uptake by human intestinal Caco-2 cells. *Am. J. Physiol. Cell Physiol.* **2001**, *281*, C1106–1117.
(37) Huh, E. C.; Hotchkiss, A.; Brouillette, J.; Glahn, R. P. Carbohydrate fractions from cooked fish promote iron uptake by Caco-2 cells. *J. Nutr.* **2004**, *134*, 1681–1689.
(38) Linder, M. C.; Zerounian, N. R.; Moriya, M.; Malpe, R. Iron and copper homeostasis and intestinal absorption using the Caco2 cell model. *Biometals* **2003**, *16*, 145–160.
(39) Oikeh, S. O.; Menkir, A.; Maziya-Dixon, B.; Welch, R. M.; Glahn, R. P. Assessment of iron bioavailability from twenty elite late-maturing tropical maize varieties using an in vitro digestion/Caco-2 cell model. *J. Sci. Food Agric.* **2004**, *84*, 1202–1206.
(40) Peng, I.-W.; Kuo, S.-M. Flavonoid structure affects the inhibition of lipid peroxidation in Caco-2 intestinal cells at physiological concentrations. *J. Nutr.* **2003**, *133*, 2184–2187.
(41) Salvini, S.; Charbonnier, M.; Defoort, C.; Alquier, C.; Lairon, D. Functional characterization of three clones of the human intestinal Caco-2 cell line for dietary lipid processing. *Br. J. Nutr.* **2002**, *87*, 211–217.
(42) Salovaara, S.; Sandberg, A.-S.; Andlid, T. Combined impact of pH and organic acids on iron uptake by Caco-2 cells. *J. Agric. Food Chem.* **2003**, *51*, 7820–7824.
(43) Wortley, G.; Leusner, S.; Good, C.; Gugger, E.; Glahn, R. Iron availability of a fortified processed wheat cereal: a comparison of fourteen iron forms using an in vitro digestion/human colonic adenocarcinoma (Caco-2) cell model. *Br. J. Nutr.* **2005**, *93*, 65–71.
(44) Zerounian, N. R.; Linder, M. C. Effects of copper and ceruloplasmin on iron transport in the Caco 2 cell intestinal model. *J. Nutr. Biochem.* **2002**, *13*, 138–148.
(45) Bissonnette, P.; Gagne, H.; Coady, M. J.; Benabdallah, K. Kinetic separation and characterization of three sugar transport modes in Caco-2 cells. *Am. J. Physiol.* **1996**, *33*, G833.
(46) During, A.; Harrison, E. H. Intestinal absorption and metabolism of carotenoids: insights from cell culture. *Arch. Biochem. Biophys.* **2004**, *430*, 77–88.
(47) During, A.; Harrison, E. H. An in vitro model to study the intestinal absorption of carotenoids. *Food Res. Int.* **2005**, *38*, 1001–1008.
(48) Konishi, Y.; Hagiwara, K.; Shimizu, M. Transepithelial transport of fluorescein in Caco-2 cell monolayers and use of such transport in in vitro evaluation of phenolic acid availability. *Biosci., Biotechnol., Biochem.* **2002**, *66*, 2449–2457.
(49) Kern, S. M.; Bennett, R. N.; Needs, P. W.; Mellon, F. A.; Kroon, P. A.; Garcia-Conesa, M. T. Characterization of metabolites of hydroxycinnamates in the in vitro model of human small intestinal epithelium Caco-2 cells. *J. Agric. Food Chem.* **2003**, *51*, 7884–7891.
(50) Konishi, Y.; Hitomi, Y.; Yoshioka, E. Intestinal absorption of *p*-coumaric and gallic acids in rats after oral administration. *J. Agric. Food Chem.* **2004**, *52*, 2527–2532.
(51) Konishi, Y. Modulations of food-derived substances on intestinal permeability in Caco-2 cell monolayers. *Biosci., Biotechnol., Biochem.* **2003**, *67*, 2297–2299.
(52) Konishi, Y.; Kobayashi, S. Transepithelial transport of chlorogenic acid, caffeic acid, and their colonic metabolites in intestinal Caco-2 cell monolayers. *J. Agric. Food Chem.* **2004**, *52*, 2518–2526.
(53) Quick, T.; Ong, D. Vitamin A metabolism in the human intestinal Caco-2 cell line. *Biochemistry* **1990**, *29*, 11116–11123.
(54) Bramley, P.; Elmadfa, I.; Kafatos, A.; Kelly, F.; Manios, Y.; Roxborough, H.; Schuch, W.; Sheehy, P.; Wagner, K. H. Vitamin E. *J. Sci. Food Agric.* **2000**, *80*, 913–938.
(55) Mardones, P.; Rigotti, A. Cellular mechanisms of vitamin E uptake: relevance in α-tocopherol metabolism and potential implications for disease. *J. Nutr. Biochem.* **2004**, *15*, 252–260.
(56) Traber, M. G.; Goldberg, I.; Davidson, E.; Lagmay, N.; Kayden, H. J. Vitamin E uptake by human intestinal cells during lipolysis in vitro. *Gastroenterology* **1990**, *98*, 96–103.
(57) Traber, M. G.; Ramakrishnan, R.; Kayden, H. J. Human plasma vitamin E kinetics demonstrate rapid recycling of plasma RRR-α-tocopherol. *Proc. Natl. Acad. Sci. U.S.A.* **1994**, *91*, 10005–10008.
(58) Erdman, J. W., Jr.; Bierer, T. L.; Gugger, E. T. Absorption and transport of carotenoids. *Ann. N.Y. Acad. Sci.* **1993**, *691*, 76–85.
(59) Erdman, J. W., Jr.; Thatcher, A. J.; Hofmann, N. E.; Lederman, J. D.; Block, S. S.; Lee, C. M.; Mokady, S. 1998. All-trans *β*-carotene is absorbed preferentially to 9-*cis*-*β*-carotene, but the latter accumulates in the tissues of domestic ferrets (*Mustela putorius puro*). *J. Nutr.* **1998**, *128*, 2009–2013.
(60) During, A.; Dawson, H. D.; Harrison, E. H. Carotenoid transport is decreased and expression of the lipid transporters SR-BI, NPC1L1, and ABCA1 is downregulated in Caco-2 cells treated with ezetimibe. *J. Nutr.* **2005**, *135*, 23305–23112.
(61) During, A.; Harrison, E. H. Mechanisms of provitamin A (carotenoid) and vitamin A (retinol) transport into and out of intestinal Caco-2 cells. *J. Lipid Res.* **2007**, *48*, 2283–2294.
(62) O'Connell, O. F.; Ryan, L.; O'Brien, N. M. Xanthophyll carotenoids are more bioaccessible from fruits than dark green vegetables. *Nutr. Res. (N.Y.)* **2007**, *27*, 258–264.
(63) Ries, R. S.; Choi, H.; Blunck, R.; Bezanilla, F.; Heath, J. R. Black lipid membranes: visualizing the structure, dynamics, and substrate dependence of membranes. *J. Phys. Chem. B* **2004**, *108*, 16040–16049.
(64) Cai, L.; Eckhardt, E. R. M.; Shi, W.; Zhao, Z.; Nasser, M.; de Villiers, W. J. S.; van der Westhuyzen, D. R. Scavenger receptor class B type I reduces cholesterol absorption in cultured enterocyte Caco-2 cells. *J. Lipid Res.* **2004**, *45*, 253–262.

(65) Covey, S. D.; Krieger, M.; Wang, W.; Penman, M.; Trigatti, L. B. Against artherosclerosis in LDL receptor-negative mice involves its expression in bone marrow-derived cells scavenger receptor class B type I-mediated protection. *Arterioscler. Thromb. Vasc. Biol.* **2003**, *23*, 1589–1594.
(66) de la Llera-Moya, M.; Connely, M. A.; Drazul, D.; Klein, S. M.; Favari, E.; Yancey, P. G.; Williams, D. L.; Rothblat, G. H. Scavenger receptor class B type I affects cholesterol homeostatis by magnifying cholesterol flux between cells and HDL. *J. Lipid Res.* **2004**, *42*, 1969–1978.
(67) Ohgami, N.; Nagai, R.; Miyazaki, A.; Ikemoto, M.; Arai, H.; Horiuchi, S.; Nakayama, H. Scavenger receptor class B type I-mediated reverse cholesterol transport is inhibited by advanced glycation end products. *J. Biol. Chem.* **2000**, *276*, 13348–13355.
(68) Rong, R.; Ramachandran, S.; Penumetcha, M.; Khan, N.; Parthasarathy, S. Dietary oxidized fatty acids may enhance intestinal apolipoprotein A-I production. *J. Lipid Res.* **2002**, *43*, 557–564.
(69) Roehrich, M.-E.; Mooser, V.; Lenain, V.; Herz, J.; Nimpf, J.; Azhar, S.; Bideau, M.; Capponi, A.; Nicod, P.; Heflinger, J.-A.; Waeber, G. Insulin-secreting $\beta$-cell dysfunction induced by human lipoproteins. *J. Biol. Chem.* **2003**, *278*, 18368–18375.
(70) Kim, K.-J. Bioelectrical characteristization of cultured epithelial cell (mono)layers and excised tissues. In *Cell Culture Models of Biological Barriers*; Lehr, C. M., Ed.; Taylor and Francis: London, U.K., 2002; pp 41−51.
(71) Blanchfield, J. T.; Dutton, J. L.; Hogg, R. C.; Gallagher, O. P.; Craik, D. J.; Jones, A.; Adams, D. J.; Lewis, R. J.; Alewood, P. F.; Toth, I. Synthesis, structure elucidation, in vitro biological activity, toxicity, and Caco-2 cell permeability of lipophilic analogues of α-conotoxin MII. *J. Med. Chem.* **2003**, *46*, 1266–1272.
(72) Daugherty, A. L.; Mrsny, R. J. Transcellular uptake mechanisms of the intestinal epithelial barrier. Part 1. *Pharm. Sci. Technol. Today* **1999**, *2*, 144–151.
(73) Balimane, P. V.; Chong, S.; Morrison, R. A. Current methodologies used for evaluation of intestinal permeability and absorption. *J. Pharmacol. Toxicol. Methods* **2000**, *44*, 301–312.
(74) Hidalgo, I. J. Assessing the absorption of new pharmaceuticals. *Curr. Topics Med. Chem.* **2001**, *1*, 385–401.
(75) Marino, A. M.; Yarde, M.; Patel, H.; Chong, S.; Balimane, P. V. Validation of the 96 well Caco-2 cell culture model for high throughput permeability assessment of discovery compounds. *Int. J. Pharm.* **2005**, *297*, 235–241.
(76) Artursson, P.; Karlsson, J. Correlation between oral drug absorption in humans and apparent drug permeability coefficients in human intestinal epithelial (Caco-2) cells. *Biochem. Biophys. Res. Commun.* **1997**, *175*, 880–885.
(77) Matthias, A.; Blanchfield, J. T.; Penman, K. G.; Toth, I.; Lang, C. S.; De Voss, J. J.; Lehmann, R. P. Permeability studies of alkylamides and caffeic acid conjugates from echinacea using a Caco-2 cell monolayer model. *J. Clin. Pharm. Ther.* **2004**, *29*, 7–13.
(78) Hu, M.; Ling, J.; Lin, H.; Chen, J. Use of cell monolayers to study drug absoption and metabolism in optimization in drug discovery. Yan, Z., Caldell, G. W., Eds.; Humana Press: Totowa, NJ, 2004; p 21.
(79) Deprez, S.; Mila, I.; Huneau, J. F.; Tome, D.; Scalbert, A. Transport of proanthocyanidin dimer, trimer, and polymer across monolayers of human intestinal epithelial Caco-2 cells. *Antioxid. Redox Signal.* **2001**, *3*, 957–967.
(80) Willmann, S.; Schmitt, W.; Keldenich, J.; Lippert, J.; Dressman, J. B. A physiological model for the estimation of the fraction dose absorbed in humans. *J. Med. Chem.* **2004**, *47*, 4022–4031.
(81) Schneeman, B. O.; Gallaher, D. Effects of dietry fibre on digestive enzyme activity and bile acids in the small intestine. *Proc. Soc. Exp. Biol. Med.* **1985**, *180*, 409–414.
(82) Schneeman, B. O. Gastrointestinal physiology and function. *Br. J. Nutr.* **2002**, *88*, S159–163.
(83) Deming, D. M.; Boileau, A. C.; Lee, C. M.; Erdman, J. W., Jr. Amount of dietary fat and type of soluble fiber independently modulate postabsorptive conversion of $\beta$-carotene to vitamin A in Mongolian gerbils. *J. Nutr.* **2000**, *130*, 2789–96.
(84) Blaustein, M. P.; Kao, J. P. Y.; Matteson, D. R. *Cellular Physiology*; Elsevier/Mosby: Philadelphia, PA, 2004; pp 1176.
(85) Issachar, D.; Holland, J. F.; Sweeley, C. C. Metabolic profiles of organic acids from human plasma. *Anal. Chem.* **1982**, *54*, 29–32.
(86) Koul, H.; Ebisuno, S.; Renzulli, L.; Yanagawa, M.; Menon, M.; Scheid, C. Polarized distribution of oxalate transport systemsin LLC-PKI cells, a line of renal epithelial cells. *Am. J. Physiol. (Renal Fluid Electrolyte Physiol. 35)*, **1994**, *266*, F266–F274.
(87) Salovaara, S.; Sandberg, A.-S.; Andlid, T. Combined impact of pH and organic acids on iron uptake by Caco-2 cells. *J. Agric. Food Chem.* **2003**, *51*, 7820–7824.
(88) Nagao, A. Oxidative conversion of carotenoids to retinoids and other products. *J. Nutr.* **2004**, *134*, 237S.
(89) Medical Encyclopedia. Glucose test -blood. [online] http://www.nlm.nih.gov/medlineplus/ency/article/003482.htm#Normal%20Values, accessed Dec 3, 2008; last updated Dec 1 2008.
(90) Pauquai, T.; Bouchoux, J.; Chateu, D.; Vidal, R.; Rousset, M.; Chambaz, J.; Demignot, S. Adaptation of enterocytic Caco-2 cells to glucose modulates triacylglycerol-rich lipoprotein secretion through triacylglycerol targeting into the endoplasmic reticulum lumen. *Biochem. J.* **2006**, *15*, 393–403, 395 (Part 2).
(91) Fuse, K.; Bamba, T.; Hosoda, S. Effects of pectin on fatty acid and glucose absorption and on thickness of unstirred water layer in rat and human intestine. *Dig. Dis. Sci.* **1989**, *34*, 1109–1116.
(92) Fishman, M. L.; Cooke, P. H.; Coffin, D. R. Nanostructure of native pectin sugar acid gels visualized by atomic force microscopy. *Biomacromolecules* **2004**, *5*, 334–341.
(93) Tammela, P.; Laitinen, L.; Galkin, A.; Wennberg, T.; Heczko, R.; Vuorela, H.; Slotte, J. P.; Vuorela, P. Permeability characteristics and membrane affinity of flavonoids and alkyl gallates in Caco-2 cells and in phospholipid vesicles. *Arch. Biochem. Biophys.* **2004**, *425*, 193–199.
(94) Steinert, R. E.; Ditscheid, B.; Netze, M.; Jahreis, G. Absorption of black currant anthocyanins by monolayers of human intestinal epithelial Caco-2 cell mounted in Ussing type champbers. *J. Agric. Food Chem.* **2008**, *56*, 4995–5001.
(95) Kaldas, M. I.; Walle, U. K.; van der Woude, H.; McMillan, J. M.; Walle, T. Covalent binding of the flavonoid quercetin to human serum albumin. *J. Agric. Food Chem.* **2005**, *53*, 4194–4197.
(96) Rawel, H. M.; Meidtner, K.; Kroll, J. Binding of selected phenolic compounds to proteins. *J. Agric. Food Chem.* **2005**, *53*, 4228–4235.
(97) Baxter, N. J.; Lilley, T. H.; Haslam, E.; Williamson, M. P. Multiple interactions between polyphenolis and salivary proline rich protein repeat result in complexation and precipitation. *Biochemistry* **1997**, *36*, 5566–5577.
(98) Bravo, L. Polyphenols: chemistry, dietary sources, metabolism and nutritional significance. *Nutr Rev., Health Med. Complete* **1998**, *56*, 317–333.
(99) Hollman, P.; de Vries, J.; van Leeuwen, S.; Mengelers, M.; Katan, M. Absorption of dietary quercetin glycosides and quercetin in healthy ileostomy volunteers. *Am. J. Clin. Nutr.* **1995**, *62*, 1276–1282.
(100) Walgren, R. A.; Lin, J.-T.; Kinne, R. K. H.; Walle, T. Cellular uptake of dietary flavonoid quercetin 4′-$\beta$-glucoside by sodium-dependent glucose transporter SGLT1. *J. Pharmacol. Exp. Ther.* **2000**, *294*, 837–843.
(101) Aguilera, J. M. Why food microstructure? *J. Food Eng.* **2005**, *67*, 3–11.

**Received for review July 21, 2008. Revised manuscript received February 13, 2009. Accepted February 16, 2009.**

JF802226N